american physiological society
AMERICAN JOURNAL OF PHYSIOLOGY
CELL PHYSIOLOGY

Am J Physiol Cell Physiol 323: C1333–C1344, 2022.
First published September 19, 2022; doi:10.1152/ajpcell.00173.2022

REVIEW

Tumor Host Interactions in Metastasis

Conversation before crossing: dissecting metastatic tumor-vascular interactions in microphysiological systems

Lakyn N. Mayo[1,2,3] and Matthew L. Kutys[1,2,4]

[1]*Department of Cell and Tissue Biology, University of California San Francisco, San Francisco, California;* [2]*UCSF-UC Berkeley Joint Graduate Program in Bioengineering, University of California San Francisco, San Francisco, California;* [3]*Medical Scientist Training Program, University of California San Francisco, San Francisco, California; and* [4]*Helen Diller Family Comprehensive Cancer Center, University of California San Francisco, San Francisco, California*

Abstract

Tumor metastasis via the circulation requires crossing the vascular barrier twice: first, during intravasation when tumor cells disseminate from the primary site through proximal vasculature, and second, during extravasation, when tumor cells exit the circulation to form distant metastatic seeds. During these key metastatic events, chemomechanical signaling between tumor cells and endothelial cells elicits reciprocal changes in cell morphology and behavior that are necessary to breach the vessel wall. Existing experimental systems have provided a limited understanding of the diverse mechanisms underlying tumor-endothelial interactions during intravasation and extravasation. Recent advances in microphysiological systems have revolutionized the ability to generate miniaturized human tissues with tailored three-dimensional architectures, physiological cell interfaces, and precise chemical and physical microenvironments. By doing so, microphysiological systems enable experimental access to complex morphogenic processes associated with human tumor progression with unprecedented resolution and biological control. Here, we discuss recent examples in which microphysiological systems have been leveraged to reveal new mechanistic insight into cellular and molecular control systems operating at the tumor-endothelial interface during intravasation and extravasation.

extravasation; intravasation; microphysiological system; organ-on-chip; tumor-vascular interaction

INTRODUCTION

Metastatic dissemination of a primary tumor to distant secondary sites is achieved by the spread of tumor cells (TCs) through nearby blood or lymphatic vasculature. Whether a tumor undergoes hematogenous or lymphatic spread, the cascade begins with intravasation, during which cells migrate from the primary tumor, breach the nearby vasculature, and enter the circulation, becoming circulating tumor cells (CTCs) (1). CTCs navigate the circulatory system and eventually extravasate within distant tissues, a process where CTCs penetrate the vessel wall for a second time to exit the circulation and form potential metastatic seeds (1). Intravasation and extravasation are therefore critical rate-limiting steps in metastasis where reciprocal chemomechanical communication occurs between TCs and endothelial cells (ECs) lining the vessel walls. These two-way paracrine and juxtracrine signals elicit the dynamic changes in cell morphology and behavior necessary to navigate these key metastatic steps. Understanding the molecular control systems and associated cell behaviors operating at the tumor-endothelial interface is therefore crucial to understanding cancer progression and for the development of new therapeutic strategies to prevent metastasis. Moreover, these control systems and cell behaviors exhibit diversity across cancer subtypes and even individual patients (1, 2). Thus, a key unmet need is to elucidate these heterogeneous mechanisms to potentially predict and prevent metastasis.

Intravital imaging in animal models including mice and zebrafish has been instrumental in demonstrating the importance of TC-intrinsic and microenvironmental factors in orchestrating intravasation and extravasation events in vivo (2–6). Furthermore, intravital methods are increasingly compatible with advancements in optogenetic and fluorescence-based reporters for controlling and measuring subcellular signaling, such as Rac1 activity, during TC migration (6). Still, intravital imaging typically requires surgical implantation of an imaging window near the tissue of interest, which can introduce confounding tissue inflammation and limits studies of metastasis to accessible organs (2). In addition, capturing rare and dynamic vessel crossing events is difficult, and it is often challenging to experimentally decouple

Correspondence: M. L. Kutys (matthew.kutys@ucsf.edu).
Submitted 26 April 2022 / Revised 8 September 2022 / Accepted 13 September 2022

specific EC-TC interactions from other factors in the in vivo milieu (2, 5). Similarly, two-dimensional (2-D) in vitro models, such as TC attachment to endothelial monolayers, have elucidated biochemical signaling mechanisms of adhesion and trans-endothelial migration including homotypic N-cadherin linkages between TCs and ECs (7) and TC adhesion to endothelial selectins (8). However, these culture systems artificially impose cell-cell interfaces within stiff, planar environments lacking the critical influences of physiological blood flow, vessel architecture, and extracellular matrix (ECM) that impact metastatic spread (5, 9, 10). These model limitations are further compounded by the intrinsic heterogeneity of human tumors and the contextual importance of signaling within distinct origin tissues (1–3). Thus, identification of core mechanisms at the TC-EC interface regulating intravasation and extravasation can be accelerated by new platforms that enable interrogation of these events within physiologically representative experimental systems.

Microphysiological system (MPS) technology is a rapidly evolving field, which melds tissue engineering with microscale physics to construct physiologically relevant models of human health and disease in vitro. In general, MPSs are three-dimensional (3-D) miniaturized human tissues consisting of one or more cell types cultured within ECM with organotypic tissue architectures, either prepatterned using 3-D printing (11) or sacrificial (12–14) techniques (Fig. 1, *A* and *B*), or self-organized via boundary-directed collective cell behaviors (15–17) (Fig. 2, *A* and *B*). These tissues are typically contained within materials such as polydimethylsiloxane (PDMS), which facilitate the incorporation of microfluidic channels to control nutrient/waste exchange and apply physiologic flow and other mechanical cues (Figs. 1, *A* and *B* and 2, *A* and *B*). Thus, MPSs support the assembly of heterotypic 3-D tissues with physiological cell-cell and cell-ECM interfaces within precisely controlled chemical and mechanical microenvironments. MPSs thereby facilitate the study of complex morphogenic events with unprecedented resolution and biological control. Applications of MPSs are increasingly transitioning from proof-of-concept tissue engineering studies toward discovery biology. Here, we reinforce the capabilities of MPSs from a biological rather than an engineering perspective and discuss recent examples where, by recapitulating key architectural and environmental features of the tumor-blood vascular interface, MPSs have emerged as tractable experimental platforms to enable new mechanistic insight into cellular and molecular processes operating during intravasation and extravasation.

INTRAVASATION

The process of intravasation begins with reciprocal paracrine communication between primary tumor cells (PTCs) and adjacent vascular endothelium. Soluble factors and ECM remodeling from the primary tumor promote vascular and EC dysfunction (Fig. 1*C*). In return, EC dysfunction feeds back onto the tumor through dysregulated interstitial fluid flow and angiocrine factors (Fig. 1*D*). As PTCs invade and reach the vasculature, PTC-EC juxtracrine signaling stimulates cell behaviors necessary for transendothelial migration (TEM) and escape into the circulation (Fig. 1*E*). By precisely structuring tumors adjacent to microvessels within MPSs, these distinct stages of intravasation can be studied with increased resolution. A classic MPS design for studying intravasation is illustrated in Fig. 1, *A* and *B* (18). In this model, PTC aggregates are positioned at a specific distance from a perfused microvessel; both tissues are encapsulated within tunable ECM that is capable of being remodeled. The MPS is mounted on a glass coverslip to facilitate high-resolution immunofluorescence and/or live imaging of tissue morphodynamics. As we discuss below, recent studies have introduced biological complexity into this MPS design to capture physiological heterotypic cell-cell interfaces and signaling during intravasation across a variety of tissue and cancer types.

Tumor-Derived Signals Modulating EC Phenotype

Modulation of vascular function via tumor-derived signals is a critical early step toward intravasation (1). Tumor-induced angiogenesis often generates leaky vasculature that is susceptible to invasion. Separately, PTC paracrine and juxtracrine cues can promote EC adhesive and morphological changes that facilitate intravasation in proximal vessels (1). It remains unclear which of these processes predominates in metastasis, or how the two processes may complement each other to ultimately permit a PTC intravasation event. In recent studies, MPSs have begun to deconvolve these processes and their molecular underpinnings in different tumor and organ contexts. Indeed, the incorporation of human and murine tumors of distinct type and tissue origin can elicit varying degrees of influence over vascular density and barrier function (12, 13, 15, 19–21). These results suggest a complex interrelationship between tumor genotype, microenvironmental signals, and EC function, which, as we demonstrate in the following examples, can be decoded within MPSs.

A recent MPS constructed an organotypic, lumenized mammary epithelial duct harboring distinct human breast cancer (BC) alterations within the ErbB-PI3K-Akt pathway (*PIK3CA H1047R*, *HER2* amplification) to investigate mutation-specific effects on epithelial architecture and on an adjacent perfused human microvessel (12). Although both genetic alterations lead to invasive transitions within the mammary epithelium, only ducts harboring activating mutation in PI3Kα elicit defects in barrier function and angiogenic sprouting in the proximal vasculature (Fig. 1, *C* and *F*). Secretome analysis and functional assays revealed ducts with activating PI3Kα mutations increase IL-6 secretion, which in turn promotes vascular dysfunction and EC activation in part by remodeling vascular endothelial cadherin (VE-cadherin) adherens junctions and the associated actin cytoskeleton (Fig. 1, *C* and *F*). This study demonstrates the importance of recapitulating native tissue architectures in effectively controlling and capturing mechanistic details of tumor-vascular paracrine crosstalk and resulting morphogenic responses. Still, this system is relatively simple, containing ducts composed of epithelia with a common genetic background; it remains unknown how such signaling cascades might be influenced by the genomic and cellular heterogeneity of human breast tumors (1, 9).

To explore how tumor microenvironmental signals, including tissue-resident fibroblasts, might lead to modulation of vascular function, Offeddu et al. (19) utilized a MPS consisting of a perfused microvascular network (primary human umbilical

vein ECs, HUVECs) laden with fibroblasts (human lung fibroblasts, HLFs). They examined the effects of PTC aggregates derived from subtypes of metastatic BC on the surrounding tumor microenvironment. Paracrine signals from tumors derived from invasive subtypes (SKBR3 and MDA-MB-468) promote local increased vascular permeability, decreased vessel density, and loss of the EC glycocalyx, a charged plasma membrane coating of glycosylated proteins that can serve as both a steric, charged barrier or a mediator of adhesive interactions (16, 22). In addition, these tumors cause stromal desmoplasia

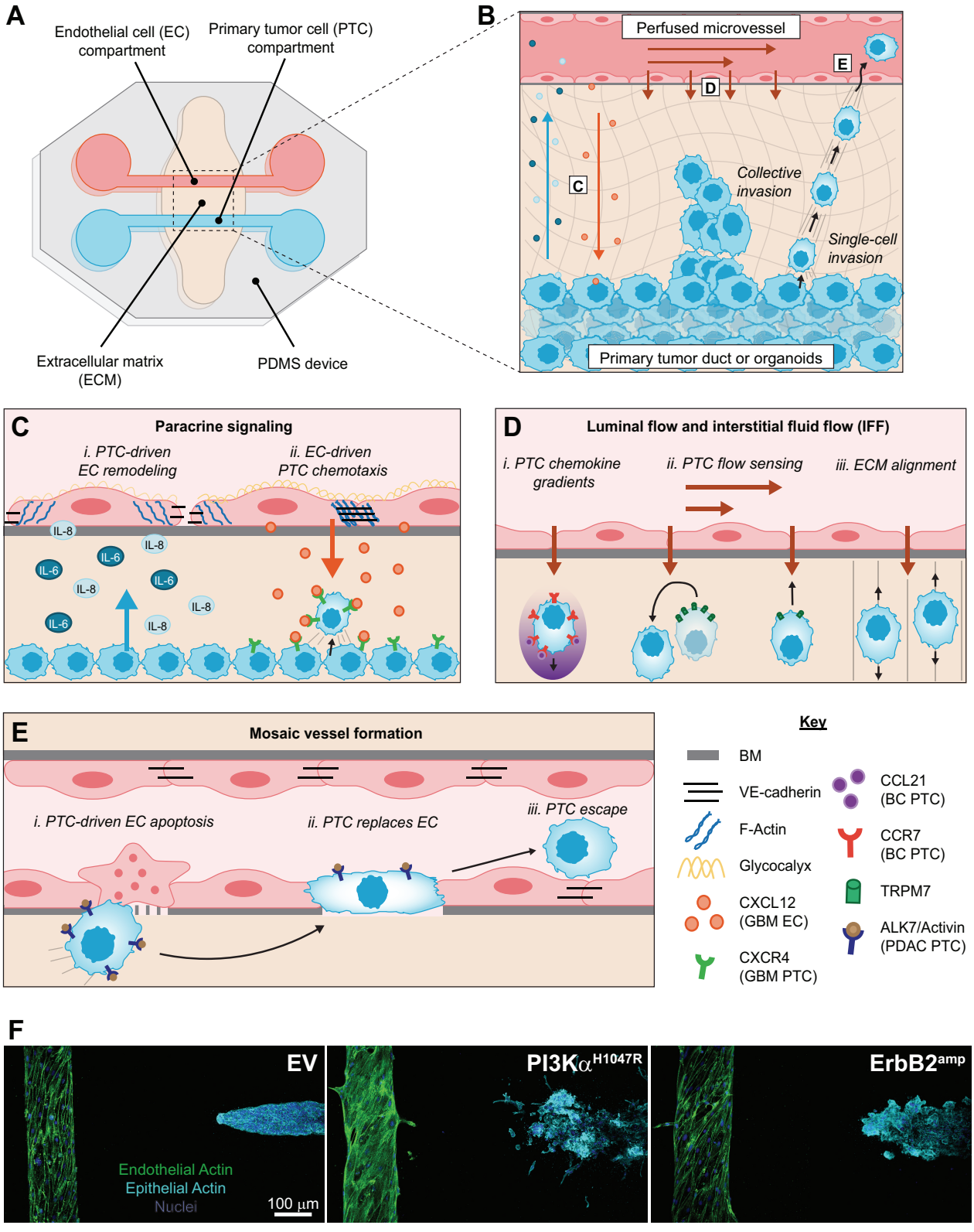

driven by triggering HLF deposition of hyaluronic acid (HA), a bulky, charged glycosaminoglycan and a marker of poor clinical BC prognosis (19), and alignment of collagen I fibers perpendicular to the tumor margin, which serve as topographical migratory cues toward the vasculature (9) (Fig. 1*D*). Here, vascular and stromal dysfunction are driven by IL-8 secretion and can be normalized by using targeted IL-8 monoclonal antibodies or broad anti-inflammatory treatments. By introducing fibroblasts, this work demonstrated how tumors might differentially leverage stromal signaling as an important intermediate in PTC-EC communication.

These studies illustrate how MPSs offer the ability to link specific mutations or tumor subtypes to functional consequences on the local microvasculature either via paracrine signaling or stromal remodeling. However, whether similar phenotypes are elicited in the presence of vascular mural cells such as pericytes is an important consideration. Although these initial mechanistic studies have focused on chemical signals conferred by paracrine communication, the impact of mechanical signals from the primary tumor on nearby vasculature, such as local solid stresses imparted by rapid tumor growth or stromal ECM deposition/stiffening (10), is underexplored in these biomimetic systems. Continually advancing techniques to monitor the evolution of tissue growth, cell-generated forces, and ECM remodeling via microscopy alongside compatibility with rheological methods will enable such studies in MPSs (5, 23, 24).

Vascular Communication at a Distance: Angiocrine Signaling and Interstitial Flow

In addition to PTC modulation of vasculature from afar, the vasculature can reciprocally regulate PTC behaviors such as stemness, trafficking, and invasion through angiocrine signaling (1, 25, 26) (Fig. 1*C*) and regulation of interstitial fluid flow (IFF; Fig. 1*D*) (10). To investigate the effects of angiocrine factors on glioblastoma multiforme (GBM) progression, Truong et al. (17) developed a microfluidic platform in which patient-derived GBM aggregates (glioma stem cells, GSCs) are fluidically connected to either a 3-D microvascular network or an acellular ECM hydrogel. Paracrine communication with vasculature enhances GSC proliferation and invasion. This was mediated, in part, by EC CXC-motif chemokine ligand 12 (CXCL12) secretion to CXC-motif chemokine receptor 4 (CXCR4) on GSCs (Fig. 1*C*). In a lung cancer MPS, where PTCs are seeded onto a semipermeable membrane gating the opening to a flow-stimulated channel, coculture with ECs on the opposite side of the membrane, stimulated increased PTC invasion across the membrane into the flow channel, though the angiocrine factors responsible remain unclear (27). Although these models importantly facilitate the isolation of endothelial paracrine effects on tumor intravasation, the imposed artificial architectures may influence angiocrine niche signaling. Truong et al. spatially separated their microvascular network from the GBM aggregates, rather than creating a physiologic tissue-tissue interface of GBM surrounded by vasculature (17). Similarly, Ni et al. examined PTC-EC communication across a 2-D polycarbonate membrane, which presents an artificial interface that may elicit aberrant EC phenotypes relative to native vessel architectures (27).

In addition to secreted factors, the endothelium impacts PTCs through regulation of interstitial fluid flow (IFF). IFF (Fig. 1, *B* and *D*) results from luminal blood pressure in capillaries pushing acellular fluid and soluble factors through the endothelium into the interstitium, which is ultimately drained by lymphatics (10). Interstitial pressure increases when this system is dysregulated—fluid incoming is too high, or lymphatic drainage is too low. Thus, the regulation of IFF is intimately tied to tumor paracrine effects: increased vascular permeability causes increased interstitial pressure (10), which has been demonstrated in MPSs (19). By precisely controlling and measuring fluid pressures and flows with microfluidics, MPSs can deconvolve the effects of IFF on PTC fate.

To begin understanding the effects of IFF on PTCs, an early MPS positioned BC (MDA-MB-231) cells in a 3-D ECM between two acellular vascular-like compartments: a higher-pressure "blood vessel" and a lower-pressure "lymphatic vessel" (28). This pressure differential within the microfluidic system generates physiologic IFF, which induces migration of PTCs, the direction of which depends on cell density and CC-motif chemokine receptor 7 (CCR7) signaling, a receptor associated with metastatic PTCs. PTCs migrate with IFF under high CCR7 stimulation via CC-motif chemokine ligand 21 (CCL21), suggesting that IFF induces an autocrine CCL21 gradient, where CCL21 concentrates downstream of PTCs under IFF (Fig. 1*D*). PTCs migrate against IFF under CCR7 inhibition and at higher cell densities, implying a competing CCR7-independent migration mechanism in response to IFF. Interestingly, this separate mechanism is mediated by upstream IFF-induced increases in focal adhesion signaling, whereby blocking Src kinase reduces IFF-directed migration. A recent study isolated the effects of vessel luminal shear

Figure 1. Microphysiological systems capture signaling and dynamic interactions at the tumor cell-endothelial interface during intravasation. *A*: example MPS device containing two separate fluidic channels embedded in 3-D ECM: one containing a perfused microvessel (top, pink) and the other containing primary tumor tissue (bottom, blue). Compartments are flanked by fluidic ports that control perfusion. *B*: zoomed-in view of MPS device, highlighting that PTCs may migrate collectively or individually to the endothelium for intravasation. *C*: bidirectional paracrine interactions between ECs and PTCs. Breast cancer (BC) cells secrete IL-6/8 to disrupt adherens junctions, actin cytoskeletal organization, and vascular glycocalyx, causing increased vascular permeability. ECs secrete CXCL12 to CXCR4 on PTCs, guiding chemotaxis toward the vasculature in GBM. *D*: luminal flow and interstitial fluid flow (IFF) regulated by ECs impacts PTC migration by *i*) generating autocrine chemokine gradients that guide PTC migration downstream; *ii*) stimulating TRPM7 channels, the expression level of which determines migration reversal or persistence; and *iii*) alignment of ECM fibers. *E*: mosaic vessel formation is one mechanism of PDAC intravasation and escape into circulation (*iii*), caused by *i*) PTC-mediated EC apoptosis and *ii*) PTC replacement of EC. *F*: maximum intensity projection images of endothelial vessels cultured nearby MCF10A ducts expressing empty vector (EV), constitutively active hemagglutinin (HA)-tagged PI3Kα H1047R (PIK3Cα^{H1047R}), or HA-tagged ErbB2 (ErbB2^{amp}) (12). PIK3Cα^{H1047R} duct causes a significant shift in endothelial actin organization from junction-associated to diffuse and cytoplasmic. Green = endothelial actin, cyan = epithelial actin, blue = nuclei; scale = 100 μm. *F* reprinted from Kutys et al. (12) with slight modifications to font sizes and text locations (Creative Commons CC BY license). BM, basement membrane; ECs, endothelial cells; ECM, extracellular matrix; GBM, glioblastoma multiforme; MPS, microphysiological system; PDAC, pancreatic ductal adenocarcinoma; PTC, primary tumor cell.

stresses and resultant IFF on fibrosarcoma (HT-1080) intravasation (29). In this MPS, PTCs are seeded into a microfluidic channel, which models the interstitium proximal to a blood vessel, and this channel is connected fluidically to a separate parallel acellular "blood vessel" channel by orthogonal microchannels. Luminal flow is applied through the blood vessel channel by hydrostatic pressure, resulting in IFF through the orthogonal microchannels. The microchannels

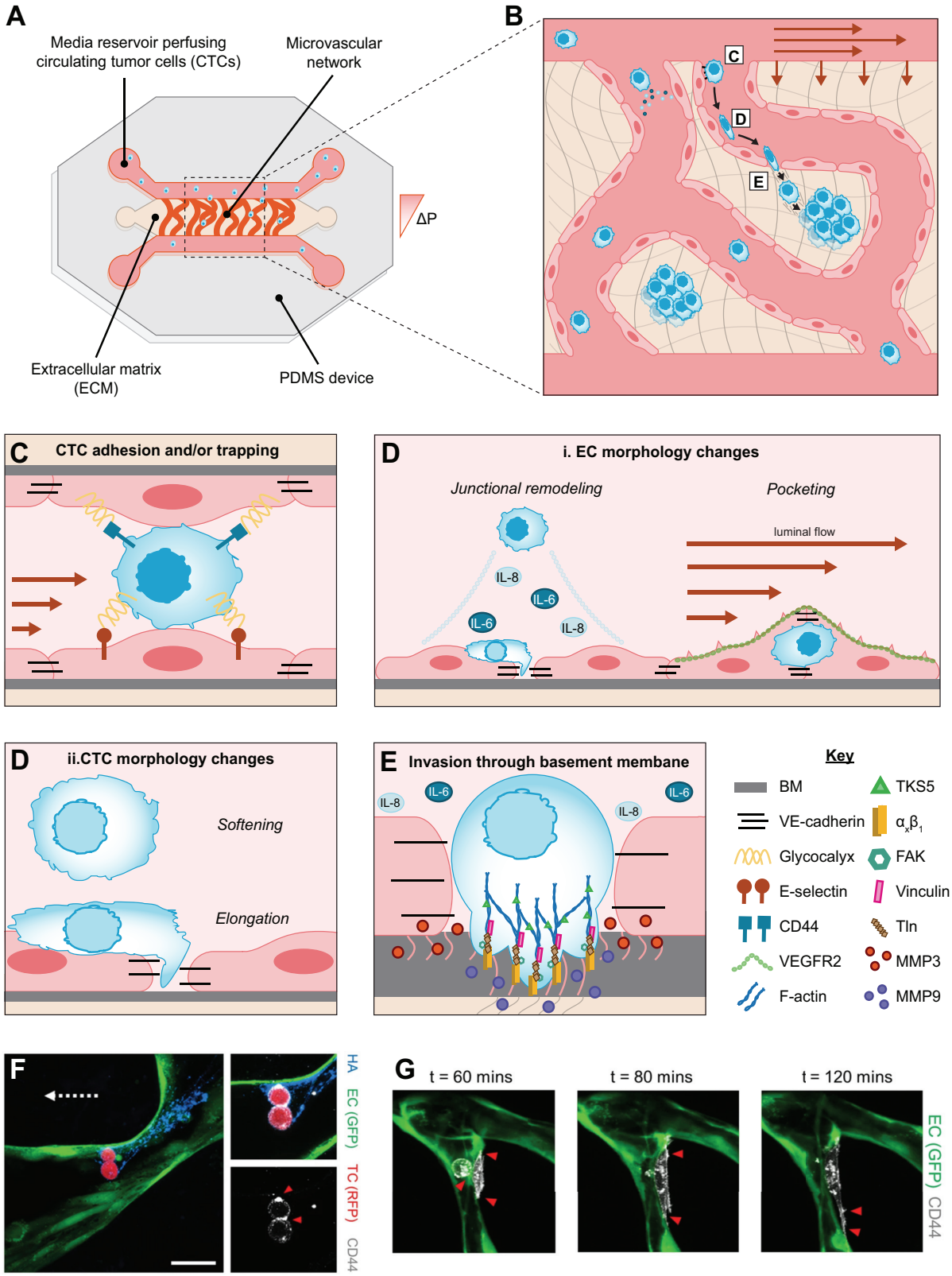

also serve as tracks for cells to invade into higher-pressure blood vessel, approximating the mechanical barriers of IFF and vessel shear stresses during intravasation. Under physiologic shear stress (0.5 or 5 dyn/cm^2), noncancerous fibroblasts tend to migrate toward the vessel channel, but on reaching the channel, reverse their migration and ultimately fail to intravasate. This migratory reversal is driven by mechanosensation of vessel shear stresses: Ca^{2+} enters the cell at the leading edge via transient receptor potential melastatin 7 (TRPM7) and the increased Ca^{2+} causes local activation of RhoA to coordinate a reversal in migratory polarity (Fig. 1*D*). Cdc42 is further activated through calmodulin/IQGAP1 and redistributed to the former trailing edge where it propagates the polarity reversal. Both pathways were elegantly interrogated by integrating optogenetic activation of RhoA or Cdc42 at either end of the cell during intravasation within the MPS. Contrasting normal fibroblasts, fibrosarcoma cells express significantly less TRPM7 and can intravasate under applied shear stress (Fig. 1*D*), which was confirmed in vivo in a chicken chorioallantoic membrane (CAM) model. Altogether, these works demonstrate that fluidic forces can influence PTC migration, the direction of which depends on a delicate interplay between IFF magnitude, specific secreted chemokines, mechanosensitive ion channels, and adhesion molecules expressed by PTCs. Though these MPSs lack the contribution of ECs, they represent important first steps in mechanistically isolating signaling responses to IFF and circulatory shear stresses independent of angiocrine factors that may influence PTC migration and intravasation.

Recent applications of MPSs have further examined the influences of IFF, ECM architecture, and their reciprocal interactions on PTC migration. By leveraging methods to apply calibrated IFF while carefully controlling ECM topography, alignment, and porosity, distinct synergistic effects on PTC migration have been described in MPSs (30–32). For example, IFF actively aligns collagen fibers (30, 33) (Fig. 1*D*) and higher ECM porosity impacts the effective IFF that cells experience (31), both of which impact PTC migration. Furthermore, the relationship between the fluidic and ECM microenvironments, PTCs, and ECs is highly intertwined: PTC-mediated vascular barrier dysfunction increases IFF, and PTCs themselves can remodel their surrounding ECM to guide migration. Thus, a critical next step for MPSs is to understand how IFF mechanotransduction at the plasma membrane or focal adhesions in PTCs dynamically interact with local ECM properties to promote PTC invasion.

Juxtracrine Communication between Tumor and Endothelial Cells

The dynamic crosstalk between PTCs and ECs at a distance ultimately results in invading PTCs contacting vessels before intravasation (Fig. 1, *B* and *E*). Intravasation requires morphological changes in both PTCs and ECs that are coordinated by juxtracrine chemomechanical signaling at the heterotypic cell-cell interface (1, 2, 18), the mechanics of which, to date, have been difficult to appreciate in vivo. The ability to capture tumor-endothelial interfaces in MPSs with high spatiotemporal resolution has shed light on dynamic single-cell and collective behaviors that drive this final step of intravasation. To capture dynamic PTC-EC juxtracrine interactions in pancreatic ductal adenocarcinoma (PDAC), Nguyen et al. (14) constructed two parallel channels: one duct formed from primary mouse PDAC cells and one lumenized microvessel within 3-D collagen ECM (Fig. 1, *A* and *B*). Stimulated by chemotactic gradients from the microvessel, the PDAC duct invades via branched structures that collectively migrate toward the vessel and then wrap around the vessel on initial contact. Following wrapping, PTCs physically occupy sites within the vessel that coincides with induced apoptosis of nearby ECs, generating a "mosaic vessel" (Fig. 1*E*), which has been observed in human PDAC tumors postmortem (14). Mechanistically, this EC apoptosis and replacement by PTCs are controlled via transforming growth factor-β (TGFβ) signaling, specifically PTC autocrine secretion of activin and binding to activin receptor-like kinase 7 (ALK7; Fig. 1*E*). To investigate PTC-EC contact during intravasation in BC, Silvestri et al. (13) placed primary mouse mammary tumor explants adjacent to a perfused microvessel (Fig. 1, *A* and *B*). Akin to the previous study, most PTCs intravasate via mosaic vessel formation, which leads to endothelial basement membrane (BM) degradation in areas occupied by PTCs. However, two additional morphogenic phenomena were observed: vessel pulling by tumor explants, or vessel constriction by the explants, the latter causing decreased or blocked vessel perfusion. These active remodeling mechanisms may contribute to vascular abnormalities, such as dead-ends, tortuosity, and irregular vessel diameters, observed in human tumors (34). Although this MPS lacks native breast tissue architecture, the relatively high-throughput nature of explant cultures enabled the observation of less common intravasation behaviors. Taken together, these studies highlight the utility of engineered vasculature to reveal new insight into diverse mechanisms of tumor-vessel

Figure 2. Microphysiological systems capture signaling and dynamic interactions at the tumor cell-endothelial interface during extravasation. *A*: example MPS device containing a microvascular network (red) flanked by two parallel media compartments (pink). ΔP = pressure differential generated across the network. CTCs (blue) are perfused. *B*: zoomed-in view of microvascular network, highlighting key paracrine and juxtracrine steps during extravasation. *C*: CTC adherence to vessel walls. This occurs by adhesion signaling (EC E-selectin to CTC glycocalyx, EC glycocalyx to CTC CD44) and/or physical trapping where the CTC is wider in diameter than the microvessel. *D*: morphological behaviors in ECs and CTCs required for extravasation: *i*) ECs remodel their junctions in response to IL-6/8 to facilitate diapedesis, or remodel their apical membrane in response to luminal flow to facilitate CTC pocketing; *ii*) CTCs soften their cell body and nuclei, and elongate along the vessel surface to facilitate migration through ECs. *E*: CTCs utilize invadopodia and EC-mediated BM destruction to facilitate invasion. CTC-expressed IL-6/8 cause ECs to express MMP3. CTC invadopodia form focal adhesions with basement membrane via $\alpha_x\beta_1$, FAK, vinculin, and talin, the latter two facilitating local actin polymerization. Invadopodia recruit Tks5 and secrete MMP9 to cause BM destruction. *F*: MDA-MB-231 BC CTCs (red) adhered to endothelium (green) through interactions between CTC CD44 (red arrows) and streaks of HA atop ECs (blue). Dashed arrow indicates direction of flow. Scale bar 60 μm (16). *G*: time-lapse confocal imaging of MDA-MB-231 overexpressing fluorescent CD44 (gray) extravasating through endothelium. Red arrows indicate regions where CD44 binds ECM. *T* = 0 min is onset of CTC perfusion (16). *F* and *G* reprinted from Offeddu et al. (16) with no modifications (Creative Commons CC BY license). BC, breast cancer; BM, basement membrane; CTC, circulating tumor cell; EC, endothelial cell; ECM, extracellular matrix; GFP, green fluorescent protein; HA, hyaluronic acid; MPS, microphysiological system PDMS, polydimethylsiloxane; RFP, red fluorescent protein; TC, tumor cell.

interactions. Given the mechanical nature of these phenomena and the supraphysiologic diameter of engineered vessels currently achievable in MPSs, it will be crucial to observe and quantitate these distinct mechanisms across a physiologic range of vessel diameters. The precise biochemical and mechanical signaling orchestrating these distinct processes remain unclear, but live imaging of these dynamic events in MPSs will continue to unravel key drivers.

EXTRAVASATION

Once a PTC successfully intravasates, it becomes a circulating tumor cell (CTC). CTCs traverse several key steps to successfully extravasate and colonize the metastatic site (1, 35). After adhering to the endothelium through active adhesion and/or confinement by vessel architecture (Fig. 2*C*), ECs remodel to allow CTCs access to the subendothelial BM, while in turn CTCs modulate their mechanics and morphology to facilitate squeezing through the constricted space of the endothelium (Fig. 2*D*). CTCs must then form stable adhesions and utilize invadopodia to breach the BM and invade the interstitium (Fig. 2*E*). Each of these discrete events, while challenging to isolate in vivo, can be recapitulated within MPSs, and recent applications have begun to assess driving mechanisms with high resolution and biological control.

3-D perfusable microvascular networks generated within MPSs facilitate the study of CTC extravasation in organotypic settings, a classic example of which is shown in Fig. 2, *A* and *B* (16). In general, ECs seeded within compliant ECM containing, or fluidically connected to, stromal fibroblasts will progressively assemble into a network of vessels with near-physiologic diameters. Microfluidic connection via the MPS to the lumenized vessel network permits perfusion of CTCs. Circulating CTCs can interact with endothelium lining the microvessels and ultimately extravasate into the interstitium. In the following sections, we discuss how recent studies have employed or adapted this MPS form for diverse tissue types and utilized novel characterization techniques to expand our knowledge of the molecular control systems operating at the CTC-blood EC interface during extravasation.

Circulating Tumor Cell Adhesion to the Endothelium

CTCs initially form weak adhesions to the blood vascular endothelium of a potential metastatic site (1, 35) (Fig. 2, *C* and *F*). Initial biochemical interactions include homotypic neuronal cadherin (N-cadherin) junctions between EC and CTC, as well as endothelial-selectin (E-selectin) and immunoglobulin superfamily cell adhesion molecules (CAMs) that interact with CTC adhesion proteins (1, 7, 8). Traditional 2-D in vitro monolayer culture has identified several molecules mediating adhesive CTC-EC interactions (7, 8), but MPSs have elucidated how these interactions are potentiated by fluid shear stress, vessel architectures, and stromal microenvironments.

To investigate the role of hemodynamic flow on initial CTC adhesion, several studies have utilized variations of a parallel plate flow chamber MPS consisting of an endothelial monolayer subjected to calibrated apical fluid flow containing CTCs. Though this approach lacks native vascular architectures and mechanics, it allows controlled application of shear stress along with techniques to quantitate adhesion strength between CTC-EC. An early MPS cultured human colon cancer cells within 3-D Matrigel hydrogels that were fluidically connected to EC monolayers cultured under calibrated shear flow (36). Disseminating CTCs adhere to the endothelial monolayer via CTC glycocalyx binding to E-selectin on ECs (Fig. 2*C*). Interestingly, E-selectin-based CTC adhesion efficiency is highest at an intermediate hemodynamic shear stress 3 dyn/cm^2, compared with 1 or 5 dyn/cm^2 (36). To further probe the relationship between shear flow and CTC adhesion, Follain et al. (5) utilized a parallel plate flow system that accommodated optical tweezers and live imaging to quantitate the temporal evolution of adhesive forces during the process of CTC-EC adhesion. Initial adhesion between a CTC and the endothelium withstands up to 80 pN of force, corresponding to ~450 μm/s flow. This result aligned with observations in a zebrafish extravasation model by the same group, where human CTCs cannot efficiently adhere to the endothelium beyond 400–600 μm/s of hemodynamic flow (5). Though these MPSs utilized 2-D endothelial monolayers, they illuminate biophysical principles by which local flow profiles might permit or prevent CTC adhesion and correlate with in vivo measurements under similar flow profiles. Still, considering the interplay between physical ECM properties and EC activation (37), it will be important to examine force-adhesion relationships in ECs within organotypic contexts, such as the classic microvascular network MPS (Fig. 2, *A* and *B*). In an initial attempt, a recent study examined the effects of luminal flow on CTC extravasation in a microvascular network within a fibrin hydrogel, using fluorescent beads to determine the range of luminal flow speeds when a 50 Pa pressure differential is applied (Fig. 2*A*): 50–500 μm/s (38). This pressure-driven luminal flow causes a threefold gain in extravasation efficiency compared with static conditions, but it remains unclear which specific luminal flow speeds correspond to individual extravasation events or which stage of extravasation is impacted.

Though EC interactions with CTC glycocalyx during adhesion have been described (36), CTC interactions with the EC glycocalyx have been difficult to study in vitro due to diminished thickness of the EC glycocalyx in in vitro static culture. The glycocalyx in static HUVECs measures only 20–30 nm (22), compared with 600–700 nm under flow (39); ex vivo murine EC glycocalyx ranges from 200 to 4,500 nm (40). Perfused microvascular network MPSs, such as those utilized by Offeddu et al. (16) and Beyer et al. (41), promote formation of a well-differentiated EC glycocalyx that changes during extravasation. After perfusing breast CTCs into preformed microvascular networks (Fig. 2, *A* and *B*), Offeddu et al. observed that CTCs adhere to streaks of HA present along the endothelium via the surface receptor CD44 (Fig. 2, *C* and *F*). These streaks often extend far past the location of the CTC, suggesting that a previous CTC had transiently adhered and "preseeded" the endothelium with HA to aid future CTC adhesion (16). In addition, CD44 may mediate interactions between CTCs and subendothelial ECM, as protrusions with elevated CD44 localization are present at extravasating CTC-ECM contact points during live imaging (Fig. 2*G*). However, when Beyer et al. utilized lectin (*Bandeiraea Simplicifolia*) staining to label the endothelial glycocalyx, shedding of EC glycocalyx also occurs immediately before CTC extravasation (41). It is

therefore important to understand which components of the EC glycocalyx are necessary for initial CTC adhesion and how depletion might facilitate extravasation.

In addition to the "adhesive capture" mechanism of CTC arrest on the endothelium is a "physical trapping" mechanism, whereby CTCs become stuck within microvessels with calibers smaller than the CTC diameter (Fig. 2*C*). Physical trapping is impossible to investigate in 2-D and difficult in vivo, but recent MPSs permit the construction of size-appropriate biomimetic human vessel architectures to study this phenomenon. Using a 3-D microvascular network MPS, Offeddu et al. (16) observed instances of both physical trapping and adhesive capture with more CTCs arresting via physical trapping in small caliber vessels. This agrees with findings in a larval zebrafish extravasation model where 50% of cells arrest via physical trapping; however, mouse brain capillaries exhibit mostly adhesive capture mechanisms (5). Thus, MPSs have aided in the appreciation that cooperation between these two mechanisms of CTC arrest, and their impact on downstream extravasation, is likely tissue-dependent.

Endothelial Cell Morphological Changes during Extravasation

For CTCs to advance beyond initial adhesion and reach the subendothelial BM, ECs must reciprocally remodel either their cell-cell junctions to permit CTC migration paracellularly (diapedesis), or their apical cell membrane to engulf CTCs through a "pocketing" mechanism (5) (Fig. 2*D*). Recent applications of MPSs have illustrated that EC junctional remodeling can occur immediately preceding CTC extravasation. Utilizing an iPSC-derived microvessel perfused by BC CTCs, Humayun et al. (42) visualized the dynamics of direct CTC-EC interactions and analyzed conditioned media to gain insight into signaling mechanisms directing these interactions. In comparison to monoculture secretomes, metastatic (MDA-MB-231), but not poorly invasive (MCF7), BC CTCs secrete IL-6/8 on interaction with ECs (Fig. 2*D*). Perfusing either CTCs or their conditioned media in the microvessel disrupts vascular barrier function, which ultimately facilitates CTC extravasation. These intriguing observations demonstrate that BC can utilize similar signals to breach EC barrier during both intravasation and extravasation (IL-6/8; Figs. 1*C* and 2*D*) (12, 19, 42). In contrast, in an iPSC-derived microvascular network MPS that incorporated astrocytes and pericytes to model the cerebrovasculature, MDA-MB-231 CTCs extravasate absent any disruption to vascular barrier (43). This demonstrates that CTCs, even from the same primary source, can exhibit tissue-specific extravasation mechanisms. Moreover, as in the case of CTC-EC adhesive mechanisms, improving tissue fidelity within MPSs is a viable strategy to reveal tissue-specific EC morphodynamics during extravasation.

In addition to junctional remodeling, ECs can utilize a pocketing mechanism to facilitate CTC TEM (Fig. 2*D*). Iterating between a MPS and a larval zebrafish model, Follain et al. (5) utilized a parallel plate system consisting of an EC monolayer subjected to calibrated flow and circulating CTCs. Comparing high-resolution imaging of TEM dynamics in the MPS and in vivo, ECs surround single or clustered CTCs using protrusive structures that form tight connections with neighboring ECs. This engulfing behavior is flow dependent and occurs through recruitment of vascular endothelial growth factor receptor 2 (VEGFR2) to the apical membrane of ECs engulfing CTCs (Fig. 2*D*) (4). Under static conditions, engulfing behavior is not observed and CTCs only extravasate through diapedesis between EC junctions with far fewer overall extravasation events. These observations offer a potential explanation for how intermediate levels of hemodynamic flow promote CTC adhesion and downstream extravasation in comparison to static conditions.

Altogether, there are multiple methods by which ECs remodel to permit CTC extravasation. Utilization of distinct mechanisms is dependent on niche preconditioning, flow conditions, and organ tropism. As these studies demonstrate, MPSs combined with high-resolution imaging can lead to a deeper understanding of the coordinated cytoskeletal and morphological EC changes that facilitate these diverse methods of extravasation.

Tumor Cell Morphological Changes Required for Intravascular Transmigration

To navigate spatially restricted migration through ECs or between ECs, and later through the BM, CTCs must dynamically alter their morphology and mechanics. Compatibility of MPSs with live high-resolution imaging and rheological methods allows for analysis of CTC morphology and mechanical changes during extravasation. In several examples of MPSs consisting of CTCs perfused through a microvascular network or an endothelialized channel, CTCs significantly elongate during transmigration, compared with the rounded morphology of CTCs in the circulation (Fig. 2*D*) (38, 41, 44). To investigate factors in the primary tumor site that may influence CTC elongation, Azadi et al. (44) cultured TCs on PDMS substrates with varied stiffnesses before perfusing them as CTCs through a rectangular endothelialized channel bordered on one side by a 3-D collagen hydrogel. CTCs initially cultured on stiffer substrate "primary sites" demonstrate greater elongation, coinciding with an increase in CTC extravasation events into the collagen hydrogel (Fig. 2*D*). Although the primary site in this MPS was 2-D and detached from the secondary site, the observations suggest that CTCs exhibit mechanical memory of the primary tumor microenvironment that potentiates later extravasation behaviors. The observation that mechanically primed CTCs might possess a greater propensity to elongate and ultimately extravasate might also explain how physical trapping within narrow microvessels promotes successful extravasation.

In addition to cell morphology, the stiffness of CTCs is hypothesized to decrease during extravasation to enable squeezing through EC features that are smaller than the CTC cell body and nucleus. To address this question, Roberts et al. (23) placed an EC monolayer atop a collagen hydrogel, which permitted application of confocal Brillouin microscopy to optically measure the elastic modulus of CTCs before, during, and after TEM into a 3-D matrix. Three different cancer cell lines (lung carcinoma, breast carcinoma, and melanoma) soften their cell body and nuclei during and after TEM (Fig. 2*D*). The entire nuclear volume appears to soften during this process, suggesting chromatin mechanics, rather than nuclear membrane remodeling, underlies the mechanical

change. These findings coincide with an in vivo study that demonstrated soft TCs (obtained from primary tumors through microfluidic sorting) are significantly more metastatic than stiff ones; soft TCs exhibit more stemness and B-cell lymphoma 9 (BCL9) expression (45). Indeed, TC mechanical properties are dynamic and critically contribute to the extravasation process, though the underlying mechanisms are poorly defined. Investigating the temporal evolution and molecular orchestrators of CTC mechanical changes provides a new way to address an unmet need in therapeutically preventing extravasation.

Strengthening Adhesions to Facilitate Invasion through the Basement Membrane

Following initial adhesion and reciprocal cell morphology changes in both CTCs and ECs, CTCs engage mechanisms to strengthen the initially weak CTC-EC interaction and ultimately migrate through the BM to the metastatic site (1, 36, 46) (Fig. 2, *E* and *G*). It has been challenging to visualize and assess subcellular functions of key protein assemblies alongside these morphogenic changes in vivo, but recent MPS applications have characterized several. Within a 3-D microvascular network, Chen et al. (46) perfused CTCs from human breast carcinoma, human melanoma, or murine mammary carcinoma, then observed extravasation events using high-resolution microscopy. Integrin β_1 (β_1) but not β_3 is required for efficient extravasation in MPSs and in in vivo mouse lungs. To isolate the effect of β_1 on initial process of CTC adhesion, CTCs were allowed to settle onto a 2-D EC monolayer for 10, 30, or 60 min, then subjected to shear flow for 15 min. β_1-knockdown CTCs adhere with the same efficiency as wild-type CTCs after 10 min, but at longer time points, wild-type CTCs show much higher CTC adhesion along with visible protrusions accessing the subendothelial ECM. This suggests that β_1 is not required for initial adhesion to the apical side of ECs, but rather strengthening CTC adhesions to the BM to withstand shear flow in this context. However, this mechanism may not be universal for all cancer subtypes and secondary organs. β_1 knockdown decreases adhesion events in a zebrafish CTC extravasation model perfused with murine BC (D2A1) cells (5), and initial melanoma CTC adhesions form between CTC $\alpha 4\beta 1$ and EC VCAM-1 in vitro (47). $\beta 1$ knockdown also changes CTC extravasation tropism in vivo (3). Moreover, in a microvascular network MPS that incorporated platelets and neutrophils, β_3 inhibition significantly reduces breast CTC adhesion, invasion, and TEM (48). The observed differential dependence on specific integrins in CTC adhesion and extravasation suggests their relevance is highly context-dependent, contributing to the heterogeneity in molecular extravasation mechanisms conferred by primary tumors and secondary tissues.

Utilizing high-resolution imaging in their MPS, Chen et al. visualized β_1 during each stage of extravasation (46). After initial adhesion, β_1 localizes to specialized invasive protrusions called invadopodia and mediates adhesion of CTCs to the BM through $\alpha_3\beta_1$ and $\alpha_6\beta_1$ integrin heterodimer binding to laminin (Fig. 2*E*). Furthermore, the β_1- and actin-rich protrusions recruit vinculin, a focal adhesion stabilizing protein, and Tks5, an invadopodia adaptor protein, to the CTC invading edge to reinforce nascent focal adhesions and allow invadopodia-based degradation through matrix metalloproteinase (MMP) activity (Fig. 2*E*). Another microvascular network MPS has identified that CTC invadopodia require directed actin polymerization and that invadopodia tips are rich in β_1, focal adhesion kinase (FAK), and talin (Tln) (49), further demonstrating that invadopodia form specialized adhesions with the BM while ultimately degrading it via various MMPs (Fig. 2*E*) (2, 9). Interestingly, components of invadopodia may depend on tissue-specific properties of the primary tumor site: BC TCs cultured within stiffer primary sites in vitro increase invadopodia-associated MMP9 expression and extravasation efficiency (44). This further suggests that mechanical priming at the tissue origin can indeed influence CTC mechanisms of extravasation.

In addition to active degradation by CTC invadopodia, MPSs have illustrated how BM can be remodeled by EC- or macrophage-mediated mechanisms. By flowing breast CTCs within an iPSC-derived microvessel, Humayun et al. (42) showed that ECs, in response to IL-6/8 from CTCs, increase secretion of MMP3 to degrade the endothelial BM (Fig. 2*E*). Though this MPS employed a large diameter single vessel architecture, this form factor facilitated unbiased secretome analyses of ECs alone, EC/CTCs, or CTCs alone to investigate signaling pathways that were activated by heterotypic interactions. To investigate effects of circulating immune cells on BM breakdown, Kim et al. (50) utilized an MPS consisting of a rectangular endothelialized channel flanked by 3-D collagen hydrogels. This channel was perfused with monocytes before perfusion with CTCs, and circulating cell interactions with the endothelium were observed with real-time high-resolution imaging. During vascular egress, monocytes differentiate into macrophages and extravasate through the endothelium and BM using MMP9 to form local channels within the BM. CTCs can subsequently adhere and traverse through these channels during extravasation, with a greater efficiency of extravasation events and invasion distances than CTCs do alone.

Finally, signaling from stroma within the metastatic site also contributes to EC-CTC adhesion and interstitial invasion. Hajal et al. (43) constructed an MPS of BC metastasizing to the brain, incorporating pericytes and astrocytes that organized around microvasculature. In this model, astrocyte-derived CCL2 signals to CCR2 on CTCs to enhance chemotaxis through the endothelium. To study mechanisms of breast CTC extravasation to the bone or lung, Kwak et al. (51) incorporated either human bone or lung fibroblasts within ECM around a perfused microvessel. Harvested organotropic breast CTCs—MDA-MB-231 CTCs that selectively metastasized to the bone or lung in vivo—were perfused within the vessel lumen. Bone-mimetic microenvironments support the selective extravasation of bone-tropic CTCs, whereas the lung microenvironment is not selective for extravasation of either organotropic CTCs. Thus, specific chemical or mechanical factors from the secondary site microenvironment can strengthen interactions between CTCs and the endothelium, and such signals can be captured within MPSs. Furthermore, these results affirm that that CTC extravasation is not solely autonomously driven, and that cooperativity with ECs, circulating immune cells, and stromal cells can occur before or after CTCs adhere to the vascular wall.

CONCLUSIONS AND FUTURE PERSPECTIVE

Microphysiological models of tumors embedded within ECM containing functional microvasculature permit the mechanistic dissection of tumor-endothelial interactions with high spatial and temporal precision. Here, we illustrate how these models have recently been employed to provide new insight into the cellular dynamics and molecular mechanisms operating at the blood EC-TC interface during the metastatic stages of intravasation and extravasation. More broadly, the modular nature of MPSs and their compatibility with modern molecular biology techniques position them as tractable experimental models to gain high-resolution insight into how human tumor heterogeneity functions to drive aggressive cancer growth and metastasis.

Different tumor subtypes utilize diverse molecular mechanisms for breaching the vasculature, and these mechanisms are influenced by the microenvironment at both primary and metastatic sites. Accessing critical underlying molecular mechanisms in organotypic models presents new opportunities that may yield strategies to predict or prevent metastasis with new biomarkers and targeted therapeutics (48). As emphasized in this review, different mechanisms of tumor-endothelial interactions can be revealed by faithfully recapitulating key aspects of the target tissue, such as in the case of a cerebrovascular biomimetic MPS revealing that BC CTCs do not cause decreased vascular barrier function before extravasation (43). Therefore, an emerging theme is that the continued evolution of MPSs toward organotypic tissue fidelity is essential to isolating critical mechanisms behind intravasation and extravasation in specific contexts. This includes the incorporation of primary and metastatic site tissue-matched vasculature, ECM, and stromal and immune cells, appropriate 3-D tissue architectures, and inclusion of relevant fluidic and mechanical forces. However, sourcing primary human tissue-matched vasculature and stroma can be challenging due to availability and the tendency of these cells to quickly lose their identity in culture. For primary ECs, vascular barrier function and EC markers can be maintained by incorporation into native tissue conformation under shear flow (52). Furthermore, the advent and rapid improvements in iPSC technology and differentiation toward endothelial and stromal lineages may present alternative avenues (15, 43). In addition, a recent discovery demonstrated that primary HUVECs may be "reset" by transient expression of embryonic-restricted ETS variant transcription factor 2 (ETV2) and then adapt to organotypic surroundings to gain tissue-specific EC identity (53).

A critical open question is how and why tumors preferentially invade through hematogenous or lymphatic routes—whether an active process whereby certain PTCs selectively intravasate preferentially through one vessel type, or a passive process determined by vessel proximity. Moreover, lymphatic drainage significantly contributes to the interstitial pressures and flows that influence both intravasation and extravasation (10). Engineered human lymphatic vessels are increasingly being developed and characterized (54–58), including complex MPS coculture models with TCs. Indeed, MPSs containing TCs alongside lumenized lymphatic vessels have revealed that BC PTCs can alter lymphatic vessel barrier function and gene expression (57), and primary head and neck tumor-derived fibroblasts induce lymphangiogenesis in nearby lymphatic vessels in a patient-specific manner (56). The molecular drivers of these processes and their implications for intravasation is an exciting open area of study. Moving forward, careful comparisons between blood and lymphatic EC-PTC interactions in MPSs may lead to molecular profiles that predict the pattern and mechanism of intravasation and potentially aid in metastatic prevention.

As several of the platforms discussed here are commercially or readily available and utilize off-the-shelf ECM reagents, primary cells, and media, MPSs are becoming increasingly tractable experimental tools for nonengineering laboratories. Although the preclinical value of MPSs for cancer drug testing and personalized medicine is well documented (15, 19, 42), their utility in dissecting new molecular and mechanical mechanisms that operate across biological scales to drive complex morphogenic behaviors in tumor progression is increasingly being realized. Along with improvements discussed above, the continued integration with rapidly advancing mechanistic technologies such as single cell and spatiotemporal "omics" (4, 59), genomic engineering (14, 29, 59), and synthetic biology will enable unique discoveries relevant to human tumor interactions with the vasculature.

ACKNOWLEDGMENTS

The authors thank Tania Singh for critical review of the manuscript. We apologize to colleagues whose work was not mentioned due to the scope and space limitations of this review.

This article is part of the special collection "Tumor Host Interactions in Metastasis." Drs. Mythreye Karthikeyan and Nadine Hempel served as Guest Editors of this collection.

GRANTS

This work was supported by the NIH (R00CA226366 and R21AG072232) and the UCSF Program for Breakthrough in Biomedical Research.

DISCLOSURES

No conflicts of interest, financial or otherwise, are declared by the authors.

AUTHOR CONTRIBUTIONS

L.N.M. prepared figures; L.N.M. and M.L.K. drafted manuscript; L.N.M. and M.L.K. edited and revised manuscript; L.N.M. and M.L.K. approved final version of manuscript.

REFERENCES

1. **Shenoy AK**, **Lu J.** Cancer cells remodel themselves and vasculature to overcome the endothelial barrier. *Cancer Lett* 380: 534–544, 2016. doi:10.1016/j.canlet.2014.10.031.
2. **di Martino JS**, **Mondal C**, **Bravo-Cordero JJ.** Textures of the tumour microenvironment. *Essays Biochem* 63: 619–629, 2019. doi:10.1042/EBC20190019.
3. **Paul CD**, **Bishop K**, **Devine A**, **Paine EL**, **Staunton JR**, **Thomas SM**, **Thomas JR**, **Doyle AD**, **Miller Jenkins LM**, **Morgan NY**, **Sood R**, **Tanner K.** Tissue architectural cues drive organ targeting of tumor cells in zebrafish. *Cell Syst* 9: 187–206.e16, 2019. doi:10.1016/j.cels.2019.07.005.
4. **Follain G**, **Osmani N**, **Gensbittel V**, **Asokan N**, **Larnicol A**, **Mercier L**, **Garcia-Leon MJ**, **Busnelli I**, **Pichot A**, **Paul N**, **Carapito R**, **Bahram S**, **Lefebvre O**, **Goetz JG.** Impairing flow-mediated endothelial remodeling

reduces extravasation of tumor cells. *Sci Rep* 11: 1–14, 2021. doi:10.1038/s41598-021-92515-2.

5. **Follain G**, **Osmani N**, **Azevedo AS**, **Allio G**, **Mercier L**, **Karreman MA**, **Solecki G**, **Garcia Leòn MJ**, **Lefebvre O**, **Fekonja N**, **Hille C**, **Chabannes V**, **Dollé G**, **Metivet T**, **Hovsepian F**, **der Prudhomme C**, **Pichot A**, **Paul N**, **Carapito R**, **Bahram S**, **Ruthensteiner B**, **Kemmling A**, **Siemonsen S**, **Schneider T**, **Fiehler J**, **Glatzel M**, **Winkler F**, **Schwab Y**, **Pantel K**, **Harlepp S**, **Goetz JG.** Hemodynamic forces tune the arrest, adhesion, and extravasation of circulating tumor cells. *Dev Cell* 45: 33–52.e12, 2018. doi:10.1016/j.devcel.2018.02.015.
6. **Nobis M**, **Herrmann D**, **Warren SC**, **Kadir S**, **Leung W**, **Killen M**, **Magenau A**, **Stevenson D**, **Lucas MC**, **Reischmann N**, **Vennin C**, **Conway JRW**, **Boulghourjian A**, **Zaratzian A**, **Law AM**, **Gallego-Ortega D**, **Ormandy CJ**, **Walters SN**, **Grey ST**, **Bailey J**, **Chtanova T**, **Quinn JMW**, **Baldock PA**, **Croucher PI**, **Schwarz JP**, **Mrowinska A**, **Zhang L**, **Herzog H**, **Masedunskas A**, **Hardeman EC, et al.** A RhoA-FRET biosensor mouse for intravital imaging in normal tissue homeostasis and disease contexts. *Cell Rep* 21: 274–288, 2017. doi:10.1016/j.celrep.2017.09.022.
7. **Qi J**, **Chen N**, **Wang J**, **Siu C-H.** Transendothelial migration of melanoma cells involves n-cadherin-mediated adhesion and activation of the β-catenin signaling pathway. *Mol Biol Cell* 16: 4386–4397, 2005. doi:10.1091/mbc.E05-03-0186.
8. **Richter U**, **Schröder C**, **Wicklein D**, **Lange T**, **Geleff S**, **Dippel V**, **Schumacher U**, **Klutmann S.** Adhesion of small cell lung cancer cells to E- and P-Selectin under physiological flow conditions: Implications for metastasis formation. *Histochem Cell Biol* 135: 499–512, 2011. doi:10.1007/s00418-011-0804-4.
9. **Winkler J**, **Abisoye-Ogunniyan A**, **Metcalf KJ**, **Werb Z.** Concepts of extracellular matrix remodelling in tumour progression and metastasis. *Nat Commun* 11: 5120, 2020. doi:10.1038/s41467-020-18794-x.
10. **Mohammadi H**, **Sahai E.** Mechanisms and impact of altered tumour mechanics. *Nat Cell Biol* 20: 766–774, 2018 [Erratum in *Nat Cell Biol*20: 1099, 2018]. doi:10.1038/s41556-018-0131-2.
11. **Meng F**, **Meyer CM**, **Joung D**, **Vallera DA**, **McAlpine MC**, **Panoskaltsis-Mortari A.** 3D bioprinted in vitro metastatic models via reconstruction of tumor microenvironments. *Adv Mater* 31: e1806899, 2019. doi:10.1002/adma.201806899.
12. **Kutys ML**, **Polacheck WJ**, **Welch MK**, **Gagnon KA**, **Koorman T**, **Kim S**, **Li L**, **McClatchey AI**, **Chen CS.** Uncovering mutation-specific morphogenic phenotypes and paracrine-mediated vessel dysfunction in a biomimetic vascularized mammary duct platform. *Nat Commun* 11: 3377, 2020. doi:10.1038/s41467-020-17102-x.
13. **Silvestri VL**, **Henriet E**, **Linville RM**, **Wong AD**, **Searson PC**, **Ewald AJ.** A tissue-engineered 3d microvessel model reveals the dynamics of mosaic vessel formation in breast cancer. *Cancer Res* 80: 4288–4301, 2020. doi:10.1158/0008-5472.CAN-19-1564.
14. **Nguyen DHT**, **Lee E**, **Alimperti S**, **Norgard RJ**, **Wong A**, **Lee JJK**, **Eyckmans J**, **Stanger BZ**, **Chen CS.** A biomimetic pancreatic cancer on-chip reveals endothelial ablation via ALK7 signaling. *Sci Adv* 5: 1–10, 2019. doi:10.1126/sciadv.aav6789.
15. **Straehla JP**, **Hajal C**, **Safford HC**, **Offeddu GS**, **Boehnke N**, **Dacoba TG**, **Wyckoff J**, **Kamm RD**, **Hammond PT.** A predictive microfluidic model of human glioblastoma to assess trafficking of blood–brain barrier-penetrant nanoparticles. *Proc Natl Acad Sci* 119: e2118697119, 2022. doi:10.1073/pnas.2118697119.
16. **Offeddu GS**, **Hajal C**, **Foley CR**, **Wan Z**, **Ibrahim L**, **Coughlin MF**, **Kamm RD.** The cancer glycocalyx mediates intravascular adhesion and extravasation during metastatic dissemination. *Commun Biol* 4: 1–10, 2021. doi:10.1038/s42003-021-01774-2.
17. **Truong D**, **Fiorelli R**, **Barrientos ES**, **Melendez EL**, **Sanai N**, **Mehta S**, **Nikkhah M.** A three-dimensional (3D) organotypic microfluidic model for glioma stem cells – vascular interactions. *Biomaterials* 198: 63–77, 2019. doi:10.1016/j.biomaterials.2018.07.048.
18. **Zervantonakis IK**, **Hughes-Alford SK**, **Charest JL**, **Condeelis JS**, **Gertler FB**, **Kamm RD.** Three-dimensional microfluidic model for tumor cell intravasation and endothelial barrier function. *Proc Natl Acad Sci U S A* 109: 13515–13520, 2012. doi:10.1073/pnas.1210182109.
19. **Offeddu GS**, **Haase K**, **Wan Z**, **Possenti L**, **Nguyen HT**, **Gillrie MR**, **Hickman D**, **Knutson CG**, **Kamm RD.** Personalized models of breast cancer desmoplasia reveal biomechanical determinants of drug penetration (Preprint). *bioRxiv*, 2021. doi:10.1101/2021.12.12.472296.
20. **Haase K**, **Offeddu GS**, **Gillrie MR**, **Kamm RD.** Endothelial regulation of drug transport in a 3D vascularized tumor model. *Adv Funct Mater* 30: 2002444, 2020. doi:10.1002/adfm.202002444.
21. **Saha B**, **Mathur T**, **Handley KF**, **Hu W**, **Afshar-Kharghan V**, **Sood AK**, **Jain A.** OvCa-chip microsystem recreates vascular endothelium-mediated platelet extravasation in ovarian cancer. *Blood Adv* 4: 3329–3342, 2020. doi:10.1182/bloodadvances.2020001632.
22. **Potter DR**, **Damiano ER.** The hydrodynamically relevant endothelial cell glycocalyx observed in vivo is absent in vitro. *Circ Res* 102: 770–776, 2008. doi:10.1161/CIRCRESAHA.107.160226.
23. **Roberts AB**, **Zhang J**, **Raj Singh V**, **Nikolić M**, **Moeendarbary E**, **Kamm RD**, **So PTC**, **Scarcelli G.** Tumor cell nuclei soften during transendothelial migration. *J Biomech* 121: 110400, 2021. doi:10.1016/j.jbiomech.2021.110400.
24. **Foss A**, **Zanoni M**, **So WY**, **Jenkins L**, **Tosatto L**, **Bartolini D**, **Gottesman M**, **Tesei A**, **Tanner K.** Patient-derived glioblastoma cells (GBM) exhibit distinct biomechanical profiles associated with altered activity in the cytoskeleton regulatory pathway (Preprint). *bioRxiv*, 2020. doi:10.1101/2020.07.16.207233.
25. **Roy-Luzarraga M**, **Reynolds LE**, **de Luxán-Delgado B**, **Maiques O**, **Wisniewski L**, **Newport E**, **Rajeeve V**, **Drake RJG**, **Gómez-Escudero J**, **Richards FM**, **Weller C**, **Dormann C**, **Meng YM**, **Vermeulen PB**, **Saur D**, **Sanz-Moreno V**, **Wong PP**, **Géraud C**, **Cutillas PR**, **Hodivala-Dilke K.** Suppression of endothelial cell FAK expression reduces pancreatic ductal adenocarcinoma metastasis after gemcitabine treatment. *Cancer Res* 82: 1909–1925, 2022. doi:10.1158/0008-5472.CAN-20-3807.
26. **Drusbosky L**, **Gars E**, **Trujillo A**, **McGee C**, **Meacham A**, **Wise E**, **Scott EW**, **Cogle CR.** Endothelial cell derived angiocrine support of acute myeloid leukemia targeted by receptor tyrosine kinase inhibition. *Leuk Res* 39: 984–989, 2015. doi:10.1016/j.leukres.2015.05.015.
27. **Ni BS**, **Tzao C**, **Huang JH.** Plug-and-play in vitro metastasis system toward recapitulating the metastatic cascade. *Sci Rep* 9: 1–13, 2019. doi:10.1038/s41598-019-54711-z.
28. **Polacheck WJ**, **Charest JL**, **Kamm RD.** Interstitial flow influences direction of tumor cell migration through competing mechanisms. *Proc Natl Acad Sci USA* 108: 11115–11120, 2011. doi:10.1073/pnas.1103581108.
29. **Yankaskas CL**, **Bera K**, **Stoletov K**, **Serra SA**, **Carrillo-Garcia J**, **Tuntithavornwat S**, **Mistriotis P**, **Lewis JD**, **Valverde MA**, **Konstantopoulos K.** The fluid shear stress sensor TRPM7 regulates tumor cell intravasation. *Sci Adv* 7: eabh3457, 2021. doi:10.1126/sciadv.abh3457.
30. **Geiger F**, **Schnitzler LG**, **Brugger MS**, **Westerhausen C**, **Engelke H.** Directed invasion of cancer cell spheroids inside 3D collagen matrices oriented by microfluidic flow in experiment and simulation. *PLoS One* 17: e0264571, 2022. doi:10.1371/journal.pone.0264571.
31. **Tien J**, **Ghani U**, **Dance YW**, **Seibel AJ**, **Karakan MÇ**, **Ekinci KL**, **Nelson CM.** Matrix pore size governs escape of human breast cancer cells from a microtumor to an empty cavity. *iScience* 23: 101673, 2020. doi:10.1016/j.isci.2020.101673.
32. **Tien J**, **Dance YW**, **Ghani U**, **Seibel AJ**, **Nelson CM.** Interstitial hypertension suppresses escape of human breast tumor cells via convection of interstitial fluid. *Cell Mol Bioeng* 14: 147–159, 2021. doi:10.1007/s12195-020-00661-w.
33. **Ng CP**, **Swartz MA.** Mechanisms of interstitial flow-induced remodeling of fibroblast-collagen cultures. *Ann Biomed Eng* 34: 446–454, 2006. doi:10.1007/s10439-005-9067-3.
34. **Senchukova MA**, **Nikitenko N. V**, **Tomchuk ON**, **Zaitsev N. V**, **Stadnikov AA.** Different types of tumor vessels in breast cancer: morphology and clinical value. *Springerplus* 4: 512, 2015. doi:10.1186/s40064-015-1293-z.
35. **Cheng X**, **Cheng K.** Visualizing cancer extravasation: from mechanistic studies to drug development. *Cancer Metastasis Rev* 40: 71–88, 2021. doi:10.1007/s10555-020-09942-2.
36. **Shin MK**, **Kim SK**, **Jung H.** Integration of intra- and extravasation in one cell-based microfluidic chip for the study of cancer metastasis. *Lab Chip* 11: 3880–3887, 2011. doi:10.1039/c1lc20671k.
37. **Ding Y**, **Floren M**, **Tan W.** High-throughput screening of vascular endothelium-destructive or protective microenvironments: cooperative actions of extracellular matrix composition, stiffness, and structure. *Adv Healthcare Mater* 6: 1601426, 2017. doi:10.1002/adhm.201601426.
38. **Hajal C**, **Ibrahim L**, **Serrano JC**, **Offeddu GS**, **Kamm RD.** The effects of luminal and trans-endothelial fluid flows on the extravasation and tissue

invasion of tumor cells in a 3D in vitro microvascular platform. *Biomaterials* 265: 120470, 2021. doi:10.1016/j.biomaterials.2020.120470.

39. **Tsvirkun D**, **Grichine A**, **Duperray A**, **Misbah C**, **Bureau L.** Microvasculature on a chip: study of the endothelial surface layer and the flow structure of red blood cells. *Sci Rep* 7: 45036, 2017. doi:10.1038/srep45036.
40. **Megens RTA**, **Reitsma S**, **Schiffers PHM**, **Hilgers RHP**, **de Mey JGR**, **Slaaf DW**, **Oude Egbrink MGA**, **van Zandvoort MAMJ.** Two-photon microscopy of vital murine elastic and muscular arteries: Combined structural and functional imaging with subcellular resolution. *J Vasc Res* 44: 87–98, 2007. doi:10.1159/000098259.
41. **Beyer S**, **Blocki A**, **Cheung MCY**, **Wan ZHY**, **Mehrjou B**, **Kamm RD.** Lectin staining of microvascular glycocalyx in microfluidic cancer cell extravasation assays. *Life* 11: 179, 2021. doi:10.3390/life11030179.
42. **Humayun M**, **Ayuso JM**, **Brenneke RA**, **Virumbrales-Muñoz M**, **Lugo-Cintrón K**, **Kerr S**, **Ponik SM**, **Beebe DJ.** Elucidating cancer-vascular paracrine signaling using a human organotypic breast cancer cell extravasation model. *Biomaterials* 270: 120640, 2021. doi:10.1016/j.biomaterials.2020.120640.
43. **Hajal C**, **Shin Y**, **Li L**, **Serrano JC**, **Jacks T**, **Kamm RD.** The CCL2-CCR2 astrocyte-cancer cell axis in tumor extravasation at the brain. *Sci Adv* 7: 1–17, 2021. doi:10.1126/sciadv.abg8139.
44. **Azadi S**, **Tafazzoli Shadpour M**, **Warkiani ME.** Characterizing the effect of substrate stiffness on the extravasation potential of breast cancer cells using a 3D microfluidic model. *Biotechnol Bioeng* 118: 823–835, 2021. doi:10.1002/bit.27612.
45. **Lv J**, **Liu Y**, **Cheng F**, **Li J**, **Zhou Y**, **Zhang T**, **Zhou N**, **Li C**, **Wang Z**, **Ma L**, **Liu M**, **Zhu Q**, **Liu X**, **Tang K**, **Ma J**, **Zhang H**, **Xie J**, **Fang Y**, **Zhang H**, **Wang N**, **Liu Y**, **Huang B.** Cell softness regulates tumorigenicity and stemness of cancer cells. *EMBO J* 40: 1–14, 2021. doi:10.15252/embj.2020106123.
46. **Chen MB**, **Lamar JM**, **Li R**, **Hynes RO**, **Kamm RD.** Elucidation of the roles of tumor integrin β1 in the extravasation stage of the metastasis cascade. *Cancer Res* 76: 2513–2524, 2016. doi:10.1158/0008-5472.CAN-15-1325.
47. **Klemke M**, **Weschenfelder T**, **Konstandin MH**, **Samstag Y.** High affinity interaction of integrin α4β1 (VLA-4) and vascular cell adhesion molecule 1 (VCAM-1) enhances migration of human melanoma cells across activated endothelial cell layers. *J Cell Physiol* 212: 368–374, 2007. doi:10.1002/jcp.21029.
48. **Crippa M**, **Bersini S**, **Gilardi M**, **Arrigoni C**, **Gamba S**, **Falanga A**, **Candrian C**, **Dubini G**, **Vanoni M**, **Moretti M.** A microphysiological early metastatic niche on a chip reveals how heterotypic cell interactions and inhibition of integrin subunit β3impact breast cancer cell extravasation. *Lab Chip* 21: 1061–1072, 2021 [Erratum in *Lab Chip* 21: 1185, 2021]. doi:10.1039/d0lc01011a.
49. **Gilardi M**, **Bersini S**, **Valtorta S**, **Proietto M**, **Crippa M**, **Boussommier-Calleja A**, **Labelle M**, **Moresco RM**, **Vanoni M**, **Kamm RD**, **Moretti M.** The driving role of the Cdk5/Tln1/FAKS732 axis in cancer cell extravasation dissected by human vascularized microfluidic models. *Biomaterials* 276: 120975, 2021. doi:10.1016/j.biomaterials.2021.120975.
50. **Kim H**, **Chung H**, **Kim J**, **Choi DH**, **Shin Y**, **Kang YG**, **Kim BM**, **Seo SU**, **Chung S**, **Seok SH.** Macrophages-triggered sequential remodeling of endothelium-interstitial matrix to form pre-metastatic niche in microfluidic tumor microenvironment. *Adv Sci (Weinh)* 6: 1900195, 2019. doi:10.1002/advs.201900195.
51. **Kwak TJ**, **Lee E.** Rapid multilayer microfabrication for modeling organotropic metastasis in breast cancer. *Biofabrication* 13, 2020. doi:10.1088/1758-5090/abbd28.
52. **Qiu Y**, **Ahn B**, **Sakurai Y**, **Hansen CE**, **Tran R**, **Mimche PN**, **Mannino RG**, **Ciciliano JC**, **Lamb TJ**, **Joiner CH**, **Ofori-Acquah SF**, **Lam WA.** Microvasculature-on-a-chip for the long-term study of endothelial barrier dysfunction and microvascular obstruction in disease. *Nat Biomed Eng* 2: 453–463, 2018. doi:10.1038/s41551-018-0224-z.
53. **Palikuqi B**, **Nguyen DHT**, **Li G**, **Schreiner R**, **Pellegata AF**, **Liu Y**, **Redmond D**, **Geng F**, **Lin Y**, **Gómez-Salinero JM**, **Yokoyama M**, **Zumbo P**, **Zhang T**, **Kunar B**, **Witherspoon M**, **Han T**, **Tedeschi AM**, **Scottoni F**, **Lipkin SM**, **Dow L**, **Elemento O**, **Xiang JZ**, **Shido K**, **Spence JR**, **Zhou QJ**, **Schwartz RE**, **de Coppi P**, **Rabbany SY**, **Rafii S.** Adaptable haemodynamic endothelial cells for organogenesis and tumorigenesis. *Nature* 585: 426–432, 2020. doi:10.1038/s41586-020-2712-z.
54. **Chung M**, **Ahn J**, **Son K**, **Kim S**, **Jeon NL.** Biomimetic model of tumor microenvironment on microfluidic platform. *Adv. Healthcare Mater* 6: 1700196–1700197, 2017. doi:10.1002/adhm.201700196.
55. **Sato M**, **Sasaki N**, **Ato M**, **Hirakawa S**, **Sato K**, **Sato K.** Microcirculation-on-a-chip: a microfluidic platform for assaying blood-and lymphatic-vessel permeability. *PLoS One* 10: e0137301, 2015. doi:10.1371/journal.pone.0137301.
56. **Lugo-Cintrón KM**, **Ayuso JM**, **Humayun M**, **Gong MM**, **Kerr SC**, **Ponik SM**, **Harari PM**, **Virumbrales-Muñoz M**, **Beebe DJ.** Primary head and neck tumour-derived fibroblasts promote lymphangiogenesis in a lymphatic organotypic co-culture model. *EBioMedicine* 73: 103634, 2021. doi:10.1016/j.ebiom.2021.103634.
57. **Ayuso JM**, **Gong MM**, **Skala MC**, **Harari PM**, **Beebe DJ.** Human tumor-lymphatic microfluidic model reveals differential conditioning of lymphatic vessels by breast cancer cells. *Adv. Healthcare Mater*. 9: e1900925, 2020. doi:10.1002/adhm.201900925.
58. **Kim S**, **Chung M**, **Jeon NL.** Three-dimensional biomimetic model to reconstitute sprouting lymphangiogenesis in vitro. *Biomaterials* 78: 115–128, 2016. doi:10.1016/J.BIOMATERIALS.2015.11.019.
59. **Saha B**, **Mathur T**, **Tronolone JJ**, **Chokshi M**, **Lokhande GK**, **Selahi A**, **Gaharwar AK**, **Afshar-Kharghan V**, **Sood AK**, **Bao G**, **Jain A.** Human tumor microenvironment chip evaluates the consequences of platelet extravasation and combinatorial antitumor-antiplatelet therapy in ovarian cancer. *Sci Adv* 7: eabg5283, 2021. doi:10.1126/sciadv.abg5283.